Influence of Stretching on the Resilience of LLDPE Monofilaments for Application in Artificial Turf

B. Kolgjini, G. Schoukens, P. Kiekens

Department of Textiles, Ghent University, Technologiepark 907, 9052 Gent, Belgium

Received 20 January 2011; accepted 31 May 2011
DOI 10.1002/app.35014
Published online 29 November 2011 in Wiley Online Library (wileyonlinelibrary.com).

ABSTRACT: Polymeric filaments have been used successfully in artificial turf, however lack of resilience and excessive fibrillation are still the main problems encountered on artificial turf fields and especially when used for football. Resilience is the ability to recover rapidly from a deformation, especially from a bending deformation. FIFA and EN standards recognize the 0.8 m-Lisport for predicting filament behavior, but this method does not provide any information concerning the resilience of individual filaments. Furthermore, it is merely a qualitative method that only assesses the system in its entirety. The research presented in this article is twofold, first to develop a test method to assess the resilience of a single filament and to correlate with the established methodology, dynamic bending by Favimat R. Second to characterize fiber morphology and to correlate the morphology characteristics with the resilience measurements. A good correlation of the static bending with dynamic bending is obtained and both test methods provide valuable information about the influence of the processing parameters on the resilience. Dynamic scanning calorimetry, Raman and WAXS measurements clearly prove the influence of the structure and more specifically of the amorphous phase on the resilience. © 2011 Wiley Periodicals, Inc. J Appl Polym Sci 124: 4081–4089, 2012

Key words: Raman spectroscopy; draw ratio; resilience; crystallinity

INTRODUCTION

Artificial turf has been used in different sports,[1] such as rugby, tennis, golf, and cricket. During the last 10 years it has been widely accepted also in football, where the so-called third generation of football turf is now being used. The first attempts to produce "first generation" of artificial football fields started in 1966 with "Astro-Turf,"[2] based on polyamide filaments and were followed in the beginning of the 1980s by the second generation with sand infill material. This second generation was not very successful for football application. The third generation, in 1996, offered a more comfortable and softer surface for players (DBF 2006,[3] see Fig. 1). The pile layer on these fields has longer fibers that were more skin-friendly. They have longer fibers, produced from polyethylene monofilaments, sand, and rubber infill material.

The FIFA Quality concept 2009[4] describes the advantages of artificial turf systems compared with natural grass, such as being weather-independent, requiring less maintenance and providing a more homogeneous surface. Besides these clear advantages there are still some drawbacks for players, such as the inappropriate ball roll behavior.[5] This is directly caused by the pile layer of monofilaments in artificial turf. On a newly installed artificial turf system, the ball roll behavior is generally very good and even comparable with the one encountered on natural grass. After a certain time of use, a degradation of properties in the pile layer is taken place. This is frequently described as a lack of resilience of the monofilaments. Resilience is the ability of the system to recover rapidly from a bending deformation and return to the original position. A test method Favimat R[6] measures the maximum force of bending of a single monofilament for each cycle, but it is possible to do measurements only at ambient conditions. The temperatures in real fields could be higher or lower than ambient conditions. So it is necessary to develop a new test method to characterize the behavior of monofilaments in real conditions.

Monofilaments used in artificial turf are made from thermoplastic materials, namely polyolefin.[7,8] An important step in their stretching, on solid phase, is the stretching ratio and the temperature by stretching. Stretching in the solid phase will cause the structure to be highly oriented,[9,10] because of lamella rearrangement, and subsequent increase in crystallinity and amorphous ordering. Different methods, such as differential scanning calorimetry

Correspondence to: B. Kolgjini (bkolgjini@yahoo.co.uk or Blerina.kolgjini@ugent.be).

Contract grant sponsors: Erasmus Mundus Project BASILEUS.

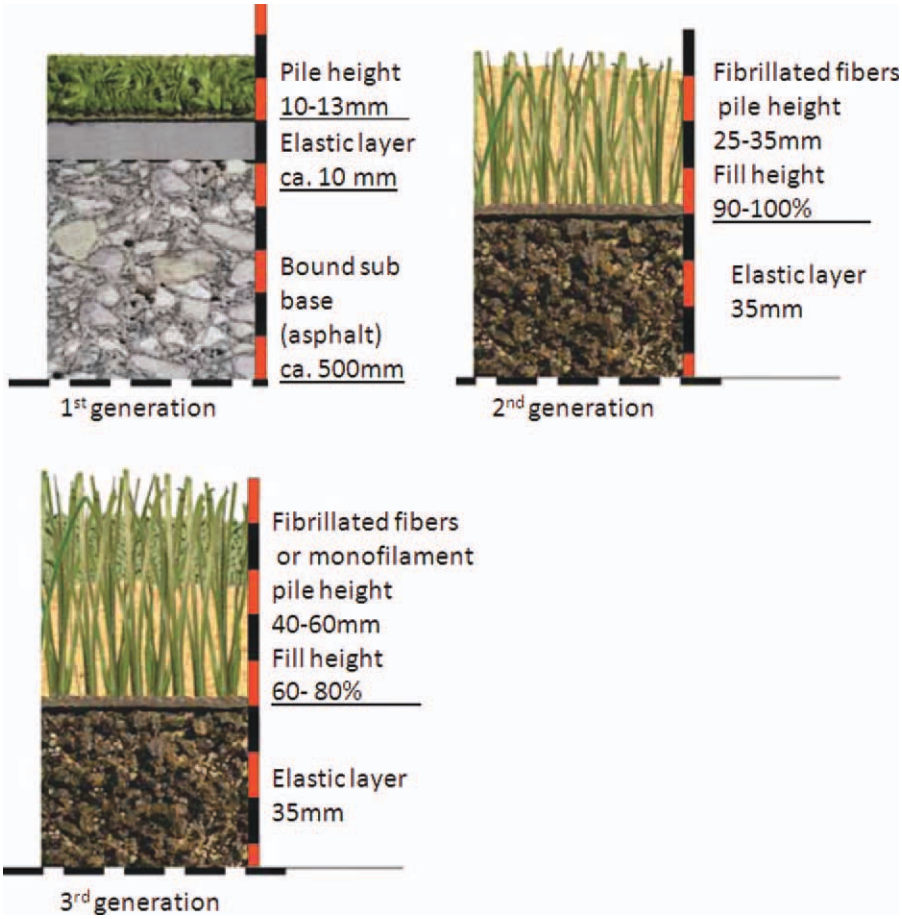

Figure 1 Development of artificial turf first generation, second generation, and third generation, (DBF 2006).[3] [Color figure can be viewed in the online issue, which is available at wileyonlinelibrary.com]

(DSC), X-ray diffraction, and Raman spectroscopy, have been used to determine the different ordered phase, such as crystallinity, and interphase of semicrystalline polymers.

This article presents the study of the influence of the processing parameters on the behavior of the filaments and more specifically on their resilience. It will be possible to predict the behavior of the filaments before producing the artificial turf and installing the entire system by realizing the measurements on a single monofilament immediately after production.

In this article, the influence of the processing parameters on the morphology of different fibers measured with DSC, X-ray, and Raman spectroscopy is correlated with the obtained resilience result.

EXPERIMENTAL

Material

The polymer material used in this study was obtained from Dow Chemical Company. DOWLEX™ 2035G,[11] linear low density polyethylene (LLDPE, Tarragona Technical Center, Tarragona Spain) with a density of 0.919 g/cm^3 and a melt index of 6 g/10 min.

Production of the monofilaments

Extrusion of monofilaments

The filaments are extruded on a Haake Polydrive Extruder by Thermo Electronic Corp. It is a single-screw extruder of 25D in length and a screw diameter of 19 mm, with a three-zone heating system. The temperature in the first section (T_1) was 140°C, in the second section (T_2) was 180°C, and the third section (T_3) was 220°C. The temperature in the die (T_4) was 220°C. The die has five diamond-shaped openings with a cross section of 2.36 mm^2 each. After the melt stage, the filaments are pulled through a water bath for producing the stretched monofilaments (see Fig. 2).

The production of monofilaments (see Fig. 2) is divided into two regions, a melt stretching region, from which is calculated the melt draw ratio (MDR) followed by a solid state stretching region, from which is calculated cold draw ratio (CDR). For the

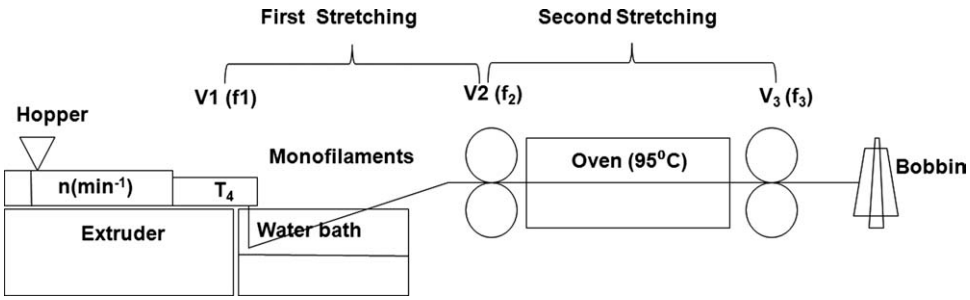

Figure 2 Schematical representation of the production of monofilaments in laboratory conditions (for symbols used, see Table I).

solid state stretching, the filaments are conditioned in an air oven at 95°C. The MDR can be calculated by dividing the cross section of the die opening (f_1 = 2.36 mm^2) with the cross section (f_2) of the filaments after the melt stretching, and CDR by dividing the cross section before (f_2) and after (f_3) solid state stretching (see Table I). The final cross section (f_3) is the same for all samples.

Monofilaments with the same cross section but different draw ratios were produced by changing the extrusion speed (v_1) and the speed of the rolls (v_2) and (v_3), (see Fig. 2). Flexing a filament will induce stress and strain that are highly influenced by the thickness of the filament. For example, doubling the thickness will, theoretically, induce a flexural stress that will be eight times higher. To avoid this thickness influence and assess only material characteristics, filaments with almost identical thickness have been tested. The influence of the thickness on resilience will be the subject of another article.

Characterization techniques

Dynamic bending test

Dynamic bending testing is performed on the Favimat R^6 (Tex Techno). The usual set up of the instrument (for tensile testing on one single filament) was modified (see Fig. 3) to be able to test resilience of one monofilament. The method consists of flexing the free side of a filament up to 300 times, during which the maximum force is monitored. The free length of the filaments is 17.5 mm, which corresponds with the average free pile length in an artificial turf system. A preload force of 0.01 cN is applied and the test speed is 100 mm/min.

The resilience is expressed as the ratio between the maximum force of the last bending cycle and the maximum force of the first bending cycle [formula (1)]. The experiment is performed at ambient conditions (23°C ± 2°C).

$$R(\%) = \frac{F_{(300)}}{F_{(1)}} \times 100 \quad (1)$$

where R is the resilience (%), F_1 is the maximum force encountered during the first cycle (cN), and F_{300} is the maximum force encountered during the last cycle, the 300th cycle (cN).

Static bending test

The static bending test is a new test method, in which monofilaments are fixed at one side, and the free side (length 17.5 mm) is bent into a straight angle of 90° (see Fig. 4).

The static bending test can be performed at different controlled temperatures and humidities by using a climate chamber, but in these experiments for

TABLE I
The Production Parameters of the Monofilaments on MDR and CDR

Sample	V_1 (m/min)	V_2 (m/min)	Tex (g/km)	f_2 (mm^2)	MDR (Ø/f_2)	V_3 (m/min)	Tex (g/km)	f_3 (mm^2)	CDR (f_2/f_3)
A_3	2.35	0.80	3045	0.66	3.52	6.09	424	0.09	7.18
A_4	2.57	0.80	2631	0.57	4.08	5.21	428	0.09	6.15
A_5	2.79	0.80	2408	0.52	4.45	4.33	424	0.09	5.68
A_6	3.01	0.80	2167	0.47	4.95	4.33	432	0.09	5.02
A_7	3.23	0.80	1883	0.41	5.70	4.00	419	0.09	4.49
A_8	3.45	0.80	1790	0.39	5.99	3.61	424	0.09	4.22
A_9	3.67	0.80	1575	0.34	6.81	3.36	429	0.09	3.67

The total stretch ratio is 25 for all samples. Melt draw ratio can also be calculeted by dividing total draw ratio with cold draw ratio.

A_3–A_9, number of samples.

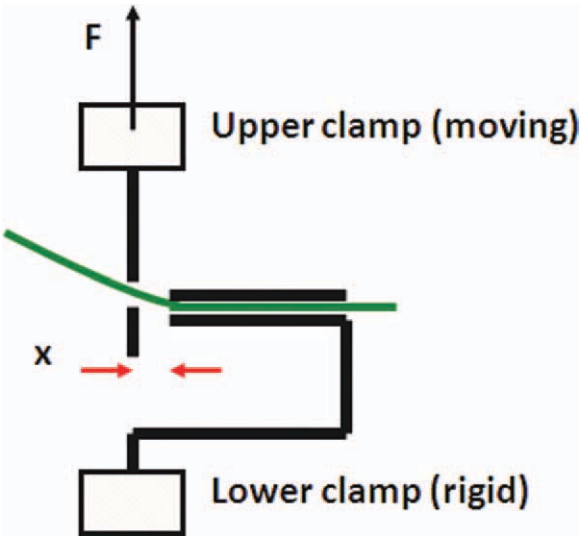

Figure 3 Schematical representation of dynamic bending test experiment Favimat R.[6] [Color figure can be viewed in the online issue, which is available at wileyonlinelibrary.com]

comparison reason with dynamic bending test the used temperature was 23°C. The recovery of the imposed deformation, defined as "deformation recovery," for each filament is calculated using formula (2) after measuring the angle between the fibers and the horizontal plate at different relaxation times: after 5 min, 1 h, 24 h, and 48 h.

$$\text{Deformation recovery}\,(\%) = \frac{\emptyset_{(t_x)}}{90} \times 100 \qquad (2)$$

where the deformation recovery is expressed in percentage (%), 90° is the maximum angle, which corresponds with the perpendicular position of the filament at the beginning (t_0), $\emptyset_{(tx)}$ is the measured value of the angle at different relaxation time(t_x), and t_x is the relaxation time (5 min, 1 h, 24 h, and 48 h).

The maximum and minimum angles of the yarn were measured for each sample and a mean value calculated. These experiments allowed to calculate the deformation recovery of the different monofilaments.

Tensile properties

The tensile tests were done on an Instron 3369, with a load cell of 500 N, samples were clamped at L = 50 mm and with a test speed v = 500 mm/min. For each sample, five replicates were tested. Tensile strength and elasticity modulus were calculated.

Differential scanning calorimetry (DSC)

DSC was performed on a DSC Q 2000 (TA Instruments), with a standard heating rate of 10°C/min in a nitrogen environment. Calibration is done with indium and tin. An enthalpy of 290 J/g for perfect crystalline polyethylene was used to calculate the percentage of crystallinity.

Raman measurements

Raman measurements were performed on a FT-Perkin–Elmer instrument. The measurements range is from 3500 to 300 cm^{-1}. Three repetitions were done for each sample, consisting of 32 scans, and a laser power of 800 mW was used. The raw Raman spectra were smoothed, and baseline corrected. The total integral intensity of the CH_2 twisting region (1250–1350 cm^{-1}) is independent from the degree of crystallinity and is used as an internal standard.[12] The mass fraction of crystalline (C_R), amorphous (A_R), and interphase (T_R) contained in the investigated samples was calculated using the formulas (3) proposed by Strobel.[12]

$$C_R = \frac{11417}{0.46 \times I_{\text{tw}}};\quad A_R = \frac{11303}{I_{tw}};\quad T_R = 1 - (C_R + A_R). \qquad (3)$$

I_{1417} and I_{1303} are the intensities at 1417 and 1303 cm^{-1}. I_{tw} is the integral intensity of the whole CH_2 twisting vibrations region (1250–1350 cm^{-1}) and was used as an internal standard.

WAXS measurements

The measurements were done on an ARL-XTRA, X-ray diffractometer from Thermo Fisher Scientific at the COMOC research group (Ghent University). Measurements are used to characterize the crystalline microscopic structure of the polymer. The radiation source Cu K_1 was operated at 45 kW 44 mA. The scanning angle ranged from 5° to 50° (2θ), λ = 1.54 Å, 0.02 step-size. The percentage of amorphous, orthorhombic crystalline phase and monoclinic phase are calculated after deconvolution of the original spectra using Gaussian fit procedure.

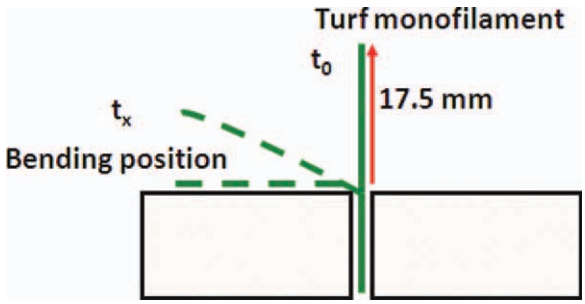

Figure 4 Schematical representation of static bending experiment. [Color figure can be viewed in the online issue, which is available at wileyonlinelibrary.com]

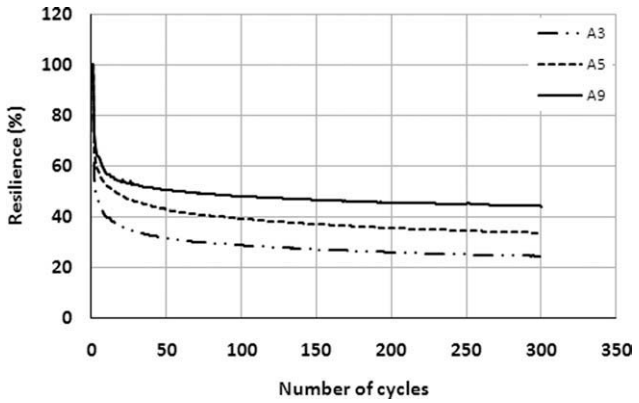

Figure 5 Resilience in function of number of bending cycles.

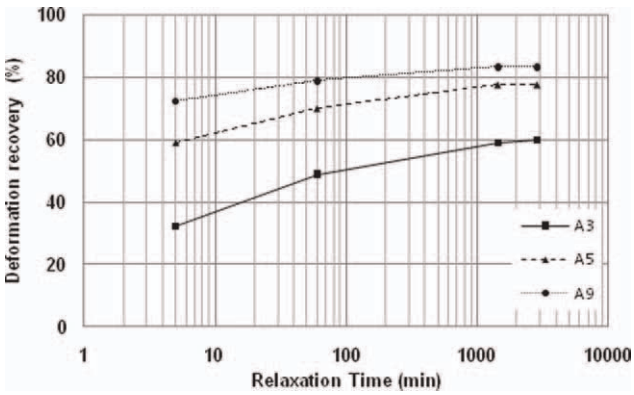

Figure 6 Deformation recovery (Static bending) versus relaxation time for samples A_3, A_5, and A_9 at ambient conditions.

RESULTS AND DISCUSSION

Optimization of the bending methods

Dynamic bending

A typical plot of the resilience as a function of number of cycles is represented in Figure 5. The monofilament resilience is decreasing with the number of bending cycles. A significant decrease occurs during the 50 first cycles and approaching a constant value afterward. A number of cycles of 300 are sufficient for obtaining the constant value of resilience.

Static bending

The deformation recovery as a function of relaxation time for three samples is represented in Figure 6: the most stretched sample (A_3), the least stretched sample (A_9) and a sample in between (A_5). The deformation recovery was constant for all samples by increasing the relaxation time from 24 to 48 h. Therefore, a time of 24 h was chosen as maximum relaxation time in further measurements.

Correlation between the two bending methods

The resilience and deformation recovery have been calculated for all the samples, using the two test methods: dynamic bending, which measures maximum force for each cycle, and static bending, which measures deformation recovery. As can be concluded from Figure 7, there is a good correlation ($R^2 = 0.93$) between the two methods.

This proves that one of two methods is sufficient to study the long time behavior of the monofilaments at laboratory conations (23°C ± 2°C), but in real conditions the temperature in the fields are different. From literatures it is well known that the polymeric materials are very much influenced by temperatures especially at higher temperatures. By performing static bending (which is more easy from technical aspects of testing) at higher temperatures and by using the found correlation with dynamic bending, it should be possible then to predict resilience at higher temperatures.

Cold drawing effect on resilience and deformation recovery

Calculations of resilience obtained by dynamic bending and deformation recovery by static bending are summarized in Table II. In Figure 8, the resilience and the deformation recovery are plotted as a function of the CDR(s).

The resilience and deformation recovery are decreasing slowly up to the CDR of 5.7, but an increase above this value of CDR, for both methods, cause a significant decrease with different gradients; the recovery deformation is more sharply decreased compared to the resilience.

This is due to different ways of acting or imposing deformation to the samples/monofilaments when comparing both methods. On dynamic bending, the samples/monofilaments are subjected to a continuous flexural deformation for 40 min and on static

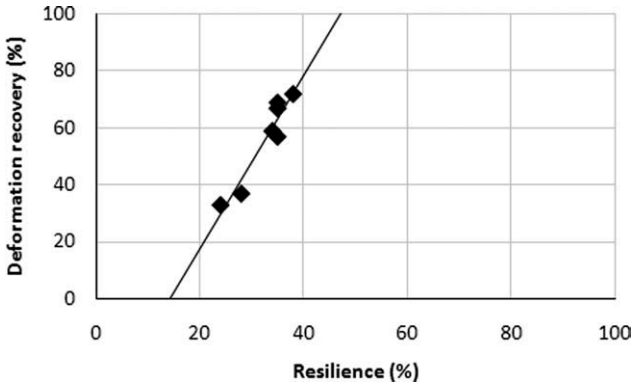

Figure 7 Plot of deformation recovery from static bending versus resilience from dynamic bending, for all the tested samples at ambient conditions.

TABLE II
Bending Behavior

Samples	Cold draw ratio	Resilience (%)	Deformation recovery (%)	DSC crystallinity (%)	DSC amorphous (%)	E Modulus (MPa)	Max load (N)
A_3	7.2	24 ± 5	33	51 ± 1	49	270 ± 3	100 ± 9
A_4	6.1	28 ± 3	37	50 ± 2	50	203 ± 8	75 ± 5
A_5	5.7	34 ± 3	59	47 ± 0	53	165 ± 9	57 ± 4
A_6	5.0	35 ± 3	57	47 ± 2	53	144 ± 6	59 ± 6
A_7	4.5	35 ± 3	69	47 ± 1	53	125 ± 4	55 ± 5
A_8	4.2	35 ± 3	67	46 ± 3	54	112 ± 4	53 ± 2
A_9	3.7	38 ± 0	72	46 ± 0	54	103 ± 3	45 ± 3

Thermal and tensile properties of samples at different CDR.

bending the deformation imposed in the samples/monofilaments is a fixed one and for 40 min.

When analyzing the differences in CDR, the possible yielding of the monofilaments is more important for the monofilaments with the high CDR (above 5.7) than the variation of the resilience, measuring the response time of the structure to the flexural deformations. This is an indication of the increased orientation of the monofilaments and the transformation of the crystalline structure into microfibrils.

As described in the literature,[13,14] the mechanical response to an applied deformation can be correlated with the morphological and molecular characteristics of the polymers. The precise morphology of an oriented sample is a function of many factors such as deformation and the process by which orientation was achieved. During the production of monofilaments two types of stretching will occur, melt stretching (initially) and solid state stretching. The melt stretching can induce a certain degree of polymer chain orientation, but an important transformation of the crystalline structure is expected by solid state stretching of the monofilaments. The orientation of crystals phase is higher than the amorphous phase, which can be explained by the easy relaxation of the amorphous chain.[15] Solid-state deformation normally results in the destruction of the crystallites of the original morphology, followed by reordering to form new crystallites.[14]

In a general way, the samples show the same behavior for both methods of bending. However, the response for static bending is more influenced by the CDR than the dynamic bending response. During static bending, the imposed deformation is constant for a relatively long period of time (40 min) and the bended filaments have the possibility to modify their structure and to create same irreversible deformation in function of the time, corresponding to same kind of yielding.

During dynamic bending, the deformations are cyclic and the measurements of the force correspond more to the response time of stress on the structure.

Correlation between bending tests and morphology structure

The values of crystalline and amorphous structures obtained by DSC, Raman, and X-ray measurements are summarized in Tables II and III. The crystalline fraction is increased by increasing CDR for all tested monofilaments, well known from literature,[13,14] but only in a limited way. Some variations are observed for the amounts of the interphase that is increased as CDR is increased. The amorphous phase measured by Raman spectra, (A_R), and DSC (see Tables II and III) is decreased by increasing CDR.

From DSC curves (see Fig. 9) it is quite clear that the melting peak temperature is around 125°C for all the samples; however, they show slightly different values of the melting enthalpy as a result of the cold drawing. The arrow in the figure indicates the results of the melting behavior on increasing CDR, going from 3.7 (A_9) to 7.2 (A_3).

By drawing above a CDR 5.7 (A_5), an increase of the DSC crystallinity is observed and the melting temperature of extra crystalline fraction is between 70 and 90°C. This is the result of the crystallization under stress or orientation of the low melting part of LLDPE, situated below the temperature of cold

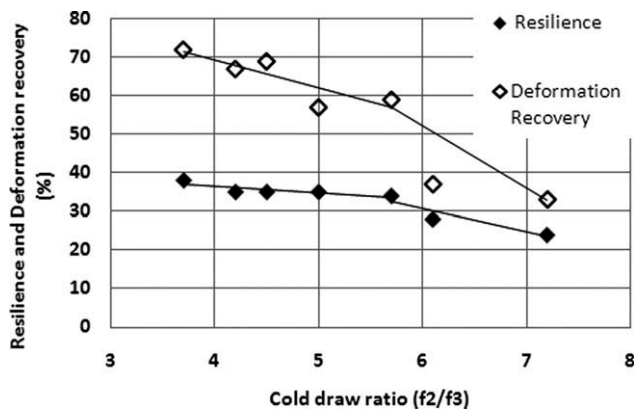

Figure 8 Deformation recovery and resilience versus CDR at ambient conditions.

TABLE III
Mass Fraction of Amorphous, Crystalline, and Interphase, Determined with Raman and WAXS Methods

		Raman			X-ray		
Sample	CDR (f_2/f_3)	Amorphous (%)	Crystalline (%)	Interphase (%)	Monoclinic crystalline (%)	Orthorhombic crystalline (%)	Amorphous (%)
A_3	7.2	36 ± 4.0	46 ± 3.1	18	16.0 ± 0.4	47.9 ± 2.2	36.0
A_4	6.2	43 ± 3.3	42 ± 4.5	15	11.4 ± 0.1	51.6 ± 1.9	36.0
A_5	5.7	46 ± 0.5	42 ± 3.3	12	9.0 ± 0.2	52.1 ± 3	38.9
A_6	5.0	47 ± 0.1	42 ± 3.3	11	11.9 ± 0.1	51.7 ± 1.7	36.3
A_7	4.5	49 ± 1.7	41 ± 3.4	10	10.8 ± 0.1	51.6 ± 2.1	37.5
A_8	4.2	50 ± 4.9	41 ± 6.6	9	12.4 ± 0.1	51.1 ± 4	36.5
A_9	3.6	51 ± 1.8	41 ± 6.0	8	11.3 ± 0.1	51.9 ± 4	36.6

drawing of the monofilament (95°C). It seems that a critical value of CDR is necessary to induce this second crystallization and to create a small concentration of very thin lamellae from the macromolecules containing a high concentration of comonomers, typical of Ziegler Natta LLDPE's.

The Raman spectra for all the samples show a typical spectrum of solid LLDPE in the 950–1500 cm^{-1} region,[16–19] by namely a superposition of three phases: an orthorhombic crystalline phase, (C_R), an amorphous phase (A_R), and a disordered phase of anisotropic nature (T_R). In Fig. 10 are represented samples A_3, A_5 and A_9. In Table IV, the assignments of the Raman bands are summarized.[19]

Comparison of the Raman spectra of these samples allowed the characterization of the monofilaments as a function of CDR. The analyzed data of the Raman measurements confirmed that the crystalline phase is not very much influenced by the CDR, a part of sample A_3 (7.2). Besides that, the so-called amorphous (A_R) and transition phases (T_R) are very much influenced, by increasing CDR; the amount of the so-called amorphous (A_R) phase is decreased while the amount of the transition phase (T_R) is increased. It follows from the discussion later on that these three phases, calculated from Raman spectra according to the published equations,[16–19] do not correspond to the different phases according to the DSC and X-ray measurements. However, a good correlation can be observed between the mechanical properties of the monofilaments and the amount of amorphous phase obtained from Raman measurements.

According to Lagaron,[20] the 1130 : 1060 cm^{-1} band intensity ratio from Raman spectrum reflects the degree of orientation. This measured ratio is increasing with the CDR and is in good correlation with the amount of transition phase. Also, the elastic modulus (see Tables II and III) is directly correlated to these ratios as presented in Figure 11 and consequently to the amount of the transition phase with a nearly constant value of the degree of crystallinity.

A good correlation ($R = 0.93$) seems to exist between the amount of amorphous phase (A_R) and deformation recovery (see Fig. 11), which confirms the correlation between the two methods presented in Figure 6. From Figure 12, the resilience and deformation recovery have the same limiting values of zero for an amount of 20% of amorphous phase, but with different limits for complete recovery or resilience. The limit for 100% resilience is obtained for a monofilament containing 100% amorphous phase and the limit for complete deformation recovery is 64% of amorphous phase.

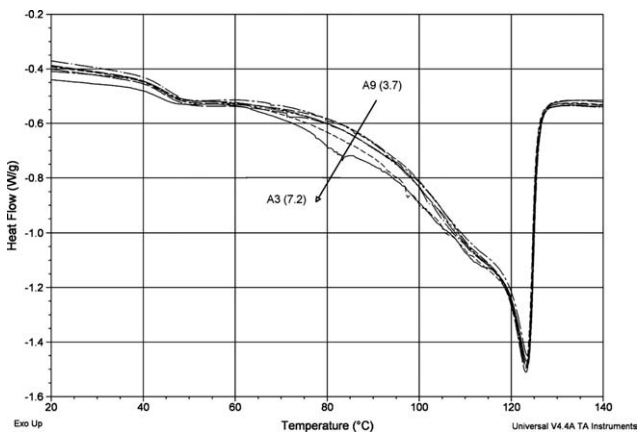

Figure 9 DSC curves of all samples with different CDR. The arrow indicates the increase of CDR.

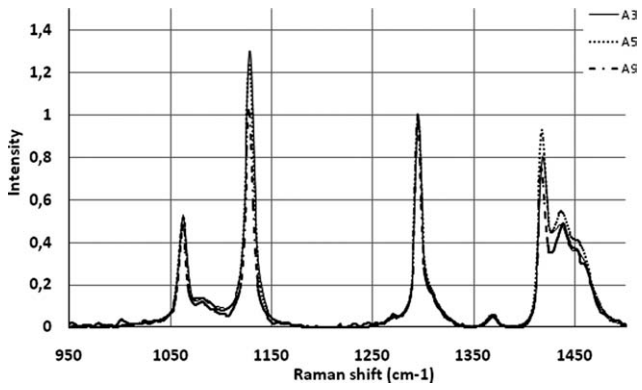

Figure 10 Raman Spectra for samples A_3, A_5, and A_9 after baseline correction and normalized at 1240–1340 cm^{-1}.

TABLE IV
Assignments of the Raman Bands of Polyethylene[16]

Bands (cm^{-1})	Phase		Mode
1060	C(A)	Vs	(C—C)
1080	A	Vs	(C—C)
1130	C(A)	Vas	(C—C)
1170	C(A)	ρ	(CH_2)
1296	C	τ	(CH_2)
1310	A	τ	(CH_2)
1370	C	ω	(CH_2)
1418	C	ω	(CH_2)
1440	A	δ	(CH_2)
1460	A	2ρ	(CH_2)

C, crystalline; A, amorphous; V, stretching [s (symmetric) and as (asymmetric)].
ρ, rocking; τ, twisting; ω, wagging; δ, bending.

From these results, a part of the amorphous phase is characterized by a zero value of resilience and deformation recovery. This means that a part of the measured amorphous phase is incorporated in the complex crystalline structure of the monofilaments and is not deformed during the bending deformations. The limit for deformation recovery is obtained for LLDPE containing 64% of amorphous phase (A_R) and 36% ordered phase (crystalline and transition phase) as measured by Raman spectroscopy with a corresponding value of resilience around 55%. As the resilience seems to be linearly influenced by the amount of amorphous phase (A_R), there is some part of the amorphous phase creating a limiting value of zero resilience after 300 cycles of dynamic bending and whose corresponding structure and force is not restored in the time scale of dynamic bending deformations.

Figure 13 represents the X-ray diffraction patterns of monofilaments obtained with different CDR. All patterns show typical orthorhombic crystal phase diffraction peaks at about 21.6°, 23.8°, and 36.3° corresponding to (110), (200), and (020) crystal planes, respectively.[21] The characteristic diffraction peaks of monoclinic crystal phase, are perceptible at 19.3°, 23.2°, and 25.1° corresponding to planes (001), (200), and (−201).

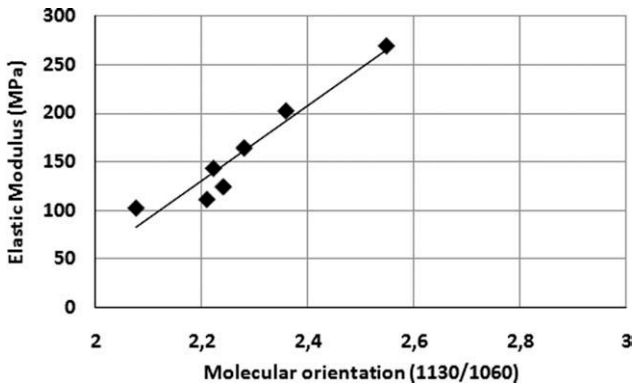

Figure 11 Elastic modulus versus molecular orientation calculated from Raman spectrum measurements.

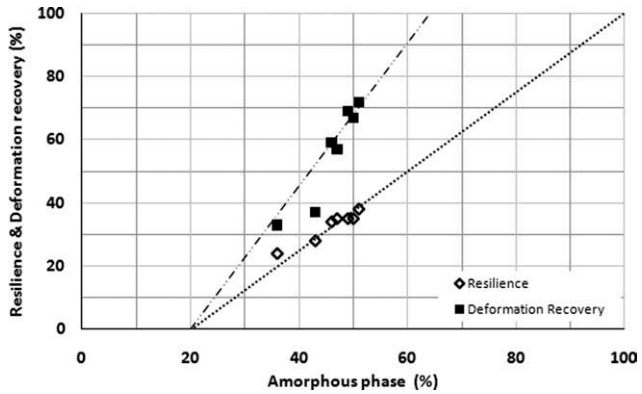

Figure 12 Resilience and deformation recovery in function of amorphous phase calculated after deconvolution of 100% Gauss curve fitting of Raman spectrum.

The calculations of the percentage of the monoclinic and orthorhombic crystalline phases are summarized in Table III. It is clear that the increase in CDR causes an increase in the percentage of orthorhombic crystalline phase until a CDR of 5.7. The amount of amorphous phase obtained by X-ray measurements is nearly constant (36%) for all the samples; however, the amount of the different crystalline structures are changing as function of the CDR. Further details of the complex structure of these different phases and differences in structures analyzed by Raman spectroscopy and X-ray measurements will be explained in a forthcoming article.

It could be concluded that the definition of amorphous phase and interphase from the Raman spectra do not correspond to the same phases according to the DSC and X-ray measurements, and that the Raman measurements are more related to the trans and gauche segments present in the oriented

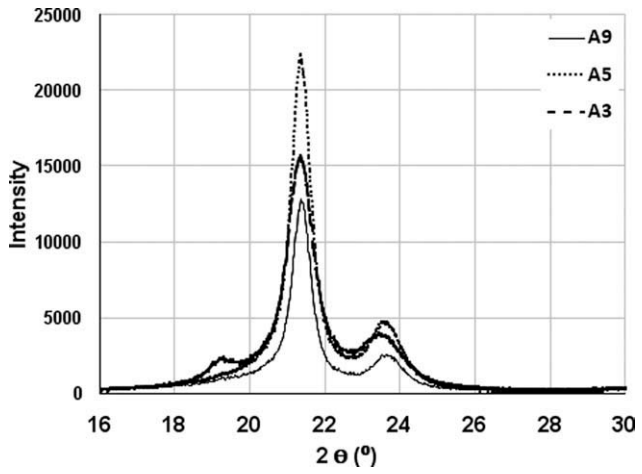

Figure 13 WAXS patterns of pellet and monofilaments with cold draw ratios 3.7 (A_9), 5.7 (A_5), and 7.2 (A_3).

monofilaments than to the different phases. Regarding the results concerning the percentage of crystallinity (see Tables II and III), different values are observed. This difference is due to the fact that different techniques have been used and that these techniques detect different types of structures.

CONCLUSIONS

The purpose of this article was to investigate the influence of the process parameters on the bending properties. Therefore two methods, which show good correlation between them, were used: deformation recovery, determined by static bending and resilience by dynamic bending. The obtained correlation between dynamic bending and static bending results can then be further used to study the resilience of the monofilaments at different temperatures, more specifically at temperatures higher than ambient temperatures.

Monofilaments produced from the same polymer and same cross section are characterized by totally different bending behavior in function of the processing parameters, specifically in function of the CDR of the monofilaments.

By increasing the CDR from 3.7 to 7.2 the tensile properties, such as the elasticity modules are increased, from 103 to 270 MPa, due to an increased amount of interphase and a decrease of amorphous phase, measured by Raman spectroscopy and also by DSC with a nearly constant amount of crystalline phase. This is a remarkable result for the correlation between the mechanical properties of the polyethylenes and the content of interphase. These results indicate that the mechanical properties of the polyethylenes are not only influenced by the degree of crystallinity, but also merely by the connections between the crystallites and by the amount and orientation in the amorphous phase as indicated by the Raman measurements.

The resilience and deformation recovery are a decrease function of the CDR of the monofilaments. The obtained results indicate that these decreases of resilience and deformation recovery are dominated by the amount of amorphous phase. Also, the influence of the amorphous phase can be split up into three parts, one part with zero values of resilience and deformation recovery, a second part with good properties of resilience and deformation recovery, and a third part with good values of deformation recovery but without resilience on the small time scale of the bending deformations. These are resulting from the complex structure of the LLDPE monofilaments obtained by the combination of melt and solid state stretching. Regarding the results concerning the amounts of the different structures, crystalline, amorphous or interphase, were observed different values from Raman spectroscopy and X-ray measurements. This difference is due to the fact that these techniques detect different types of structures, and a combination of these two techniques are necessary to obtain a complete analysis of the complex structure of the semicrystalline polymers.

The authors thank Stijn Rambour, Stefaan Janssens, and Lieve Van Landuyt for their technical support.

References

1. Schoukens, G. Chapter 5; "Development in textile sports surfaces", in Goswami, K. K., 2009, "Advanced in Carpet Manufacture", Cambridge Woodhead Publishing in Textiles, ltd.
2. Astroturf 2010. Available at http://www.astroturfusa.com/, http://www.astroturf.com. Accessed on 28 February, 2011.
3. Deutscher Fussball-Bund 2006. DFB-Empfelungen für Kunststoffrasenplätze—Fragen und Antworten. Available at http://www.dfb.de/uploads/media/DFB_Kunstrasenstudie_KF.pdf. Accessed on 25 February, 2011.
4. FIFA Quality concept for football turf 2009. Available at http://www.fifa.com/mm/document/afdeveloping/pitch&equipment/50/15/94/footballturfbookletenglish_07012009.pdf. Accessed on 28 February, 2011.
5. Joosten, T. 2003. Players experiences of artificial turf. ISSS Stadia turf summit, Amsterdam. (ISSS publication). Available at http://www.isss.de/conferences/Amsterdam2003/Joosten.pdf. Accessed on December, 2010.
6. Schoukens, G.; Rambour, S. International Conference on Latest Advances in High -Tech Textiles and Textiles-based Materials. 23–25 September (2009), Belgium.
7. Patent application EP1672020. Polyethylene composition for artificial turf (21/06/2006).
8. Patent application JP7150437. Low-crimped pile yarn for artificial turf (nylon 6 and /or nylon 66) (13/06/1995).
9. Failla, M. D.; Carrella, J. M.; De Micheli, R. J Polym Sci Polym Phys 1988, 26, 2433.
10. Clements, J.; Jakeways, R.; Ward, I. M. Polymer 1978, 19, 639.
11. DOWLEX^{TM} 2035 G (Cast Film), Polyethylene Resin. Tarragona Technical Center, Tarragona Spain.
12. Strobel, R. G.; Hagerdon, W. J Polym Sci Polym Phys Ed 1978, 16, 1181.
13. Rabiej, S.; Binias, W.; Binias, D. Fibers Text East Eur 2008, 16, 5762.
14. Peacock, A. J. Hand book of Polyethylene Structure Properties and Application; New York, 2000, Chapters 6 and 8.
15. Zuo, F.; Burger, C.; Chen, X.; Mao, Y.; Hsiao, B. S. Macromolecules 2010, 43, 1922.
16. Sato, H.; Shimoyama, M.; Kamiya, T.; Amari, T.; Šašic, S.; Ninomiya, T.; Siesler, H. W.; Ozaki, Y. J Appl Polym Sci 2002, 86, 443.
17. Lagaron, J. M. J Mater Sci 2002, 37, 4101.
18. Paradkar, R. P.; Salhalkar, S. S.; He, X.; Ellison, M. S. J Appl Polym Sci 2003, 88, 545.
19. Maxfield, J.; Stein, R. S.; Chen, M. C. J Polym Sci Polym Phys Ed 1978, 16, 37.
20. Lagaron, J. M.; Dixon, N. M.; Reed, W.; Pastor, J. M.; Kip, B. J. Polymer 1999, 40, 2569.
21. Russell, K. E.; Hunter, B. K.; Heyding, R. D. Polymer 1997, 38, 1409.